

OPEN ACCESS

EDITED BY Alice Chen, Consultant, Potomac, MD, United States

REVIEWED BY
Daw-Yang Hwang,
National Health Research Institutes, Taiwan
Jie Ding,
Peking University, China

*CORRESPONDENCE
Kar Hui Ng

☑ paenkh@nus.edu.sg
Yaochun Zhang
☑ paezyc@nus.edu.sg

RECEIVED 14 April 2025 ACCEPTED 08 September 2025 PUBLISHED 29 September 2025

CITATION

Koh CT, Lim TST, Loh AHL, Ng YF, Kwek JL, Lau PYW, Chin H-I, Ng JL, Than M, Mok IY, Lim CC, Chong KY, Choo JCJ, Yap HK, Ng KH and Zhang Y (2025) Case Report: Evaluation of *COL4A5* non-canonical splicing variants in two families. *Front. Med.* 12:1611334. doi: 10.3389/fmed.2025.1611334

COPYRIGHT

© 2025 Koh, Lim, Loh, Ng, Kwek, Lau, Chin, Ng, Than, Mok, Lim, Chong, Choo, Yap, Ng and Zhang. This is an open-access article distributed under the terms of the Creative Commons Attribution License (CC BY). The use, distribution or reproduction in other forums is permitted, provided the original author(s) and the copyright owner(s) are credited and that the original publication in this journal is cited, in accordance with accepted academic practice. No use, distribution or reproduction is permitted which does not comply with these terms.

Case Report: Evaluation of COL4A5 non-canonical splicing variants in two families

Chee Teck Koh^{1,2}, Tina Si Ting Lim^{1,2}, Alwin Hwai Liang Loh³, Yan Fei Ng³, Jia Liang Kwek⁴, Perry Yew Weng Lau^{1,2}, Hui-lin Chin^{1,2}, Jun Li Ng^{1,2}, Mya Than^{1,2}, Irene Yanjia Mok⁴, Cynthia Ciwei Lim⁴, Kay Yuan Chong⁵, Jason Chon Jun Choo⁴, Hui Kim Yap^{1,2}, Kar Hui Ng^{1,2}* and Yaochun Zhang^{1,2}*

¹Department of Paediatrics, Yong Loo Lin School of Medicine, National University of Singapore, Singapore, Singapore, ²Khoo Teck Puat-National University Children's Medical Institute, National University Health System, Singapore, Singapore, ³Department of Anatomical Pathology, Singapore General Hospital, Singapore, Singapore, ⁴Department of Renal Medicine, Singapore General Hospital, Singapore, Si

Introduction: Alport syndrome is one of the most prevalent monogenic kidney diseases, resulting from the defects in *COL4A3*, *COL4A4*, and/or *COL4A5* genes. Interpretation of non-canonical splicing variants can be challenging. This study aimed to resolve two variants at non-canonical splice sites in the *COL4A5* gene using multiple modalities.

Methods: Exome sequencing was performed on two families suspected of having Alport syndrome. Intronic splice site variants in COL4A5, which have been reported in the literature, were identified: c.1032 + 4A > G in one family and a four-nucleotide deletion, c.1032 + 3_1032 + 6delAAGT, in the other. To clarify the pathogenicity of these variants, several analyses were performed: familial co-segregation analyses in relation to comprehensive phenotyping of family members, immunofluorescence analysis of kidney biopsy specimens to evaluate collagen IV $\alpha 5$ staining patterns, and minigene splicing assay to assess the impact on pre-messenger RNA (mRNA) splicing.

Results: The family studies demonstrated co-segregation of the variants among members with characteristic phenotypic features. The immunofluorescence analysis of the kidney biopsy samples displayed aberrant collagen IV $\alpha 5$ staining patterns. The minigene splicing assay revealed that both variants caused exon 18 skipping in the *COL4A5* gene, resulting in truncated transcripts.

Conclusion: The study demonstrated a multi-faceted approach to improve the diagnostic accuracy and clinical utility of genetic testing for Alport syndrome.

KEYWORDS

Alport syndrome, COL4A5, splicing variants, minigene assay, variant interpretation

Introduction

Alport syndrome is one of the most common monogenic kidney diseases (1). It is caused by defects in the *COL4A3*, *COL4A4*, and/or *COL4A5* genes, which encode the α 3, α 4, and α 5 chains of collagen IV, respectively. Each of these chains intertwines to form a triple helix, which interconnects to form the glomerular basement membrane (GBM). Pathogenic variants in these three genes may occur as missense, deletion, insertion, nonsense, or splice site variations,

resulting in the loss of protein function or an altered protein morphology (2).

There are four forms of Alport syndrome: autosomal dominant Alport syndrome (ADAS), autosomal recessive Alport syndrome (ARAS), X-linked Alport syndrome (XLAS), and digenic Alport syndrome. Individuals with Alport syndrome can develop microhematuria in early life, and this may progress to proteinuria and subsequently chronic kidney disease (CKD). Some patients do not have classical phenotypes. Instead, they present with cystic kidneys (3-5), early-onset hypertension, or "CKD of unknown cause" (1). Patients with ARAS or XLAS may develop neurosensory hearing loss and/or ocular lesions. Characteristic electron microscopic features of Alport syndrome include splitting, scalloping, lamellation, and a basket-weaving appearance of the GBM in the kidney. Immunofluorescence analysis of collagen IV $\alpha 3$, α 4, or α 5 chains may be useful in confirming the diagnosis of Alport syndrome, as decreased or abnormal staining patterns of collagen IV $\alpha 3$, $\alpha 4$, and $\alpha 5$ can occur, depending on the genotype (6). Early and aggressive blockade of the renin-angiotensin-aldosterone system may delay kidney failure by two decades or more (7, 8). The earlier the treatment is started, the greater the impact on kidney survival (7). Alport syndrome is largely diagnosed through kidney biopsies or genetic testing. However, kidney biopsies are traditionally not clinically indicated in the early stage of the disease when only isolated microhematuria or mild albuminuria is present. Moreover, the classical histological changes associated with Alport syndrome are often not present in the early stages of the disease. Therefore, the early diagnosis of Alport syndrome—crucial for significantly improving kidney survival, primarily relies on genetic testing.

The interpretation of variants of uncertain significance (VUSs) remains a significant challenge in genomic medicine. Several additional approaches may be employed to facilitate the reclassification of a VUS into either pathogenic or benign categories. The selection of these strategies is depends on the specific characteristics of the variant, the clinical and familial context, and the available evidence from the scientific literature and genomic databases. Potential strategies may include comprehensive phenotyping of the proband or affected family members, segregation analysis through variant-specific testing in relatives, and functional studies (9, 10). Nevertheless, the implementation of these investigations in routine clinical practice is often limited by feasibility constraints or may yield inconclusive results.

Functional studies performed in the molecular laboratory may provide further information that can help re-classify the VUS, particularly when conventional clinical approaches are unfeasible or inconclusive. Specifically, the minigene splicing assay has emerged as a robust method to evaluate the effects of VUSs located at non-canonical splice sites, which are particularly challenging as there is no established consensus or approach (11–13).

In this report, we describe two unrelated families, each presenting with clinical manifestations consistent with Alport syndrome. Both families harbored a distinct non-canonical intronic splice site variant in the *COL4A5* gene, which had been classified as VUSs by commercial sequencing laboratories. We aimed to resolve these two VUSs by integrating additional lines of evidence, including the minigene splicing assay, in accordance with the guidelines established by the American College of Medical Genetics and Genomics (ACMG)/ Association for Molecular Pathology (AMP) (14).

Case description

Family A

The proband (III-3; Figure 1A), a 41-year-old Chinese woman, was first noted incidentally to have persistent microscopic hematuria at the age of 4. Urinalysis showed 40 red blood cells (RBCs) per highpower field (hpf), 45% of which were dysmorphic. She had normoalbuminuria, a normal estimated glomerular filtration rate (eGFR), and a negative autoimmune screen. The microhematuria persisted into adulthood, with urine RBC counts reaching up to 130 per hpf. By the age of 21, she had developed subnephrotic albuminuria (Kidney Disease: Improving Global Outcomes [KDIGO] category A3). Following a kidney biopsy (see Histological examination below), angiotensin-converting-enzyme inhibitor (ACE-i) therapy was initiated but subsequently discontinued at age 27 due to reproductive considerations. During her two pregnancies, her proteinuria worsened transiently, peaking at 0.35 g/day/1.73m². ACE-i treatment was reinstated after the pregnancies, resulting in stabilization of her proteinuria. At present, her eGFR remains normal, and the urine protein-to-creatinine ratio is subnephrotic at 0.04 g/mmol (normal <=0.02 g/mmol) with an angiotensin II receptor blocker (ARB) treatment (Figure 1B). A hearing check at age six was normal and has not been repeated since.

The proband's mother (II-2) was diagnosed with hypertension and probable glomerulonephritis during pregnancy. The hypertension persisted after pregnancy, but she discontinued treatment. Eventually, she developed kidney failure by the age of 60, requiring kidney replacement therapy.

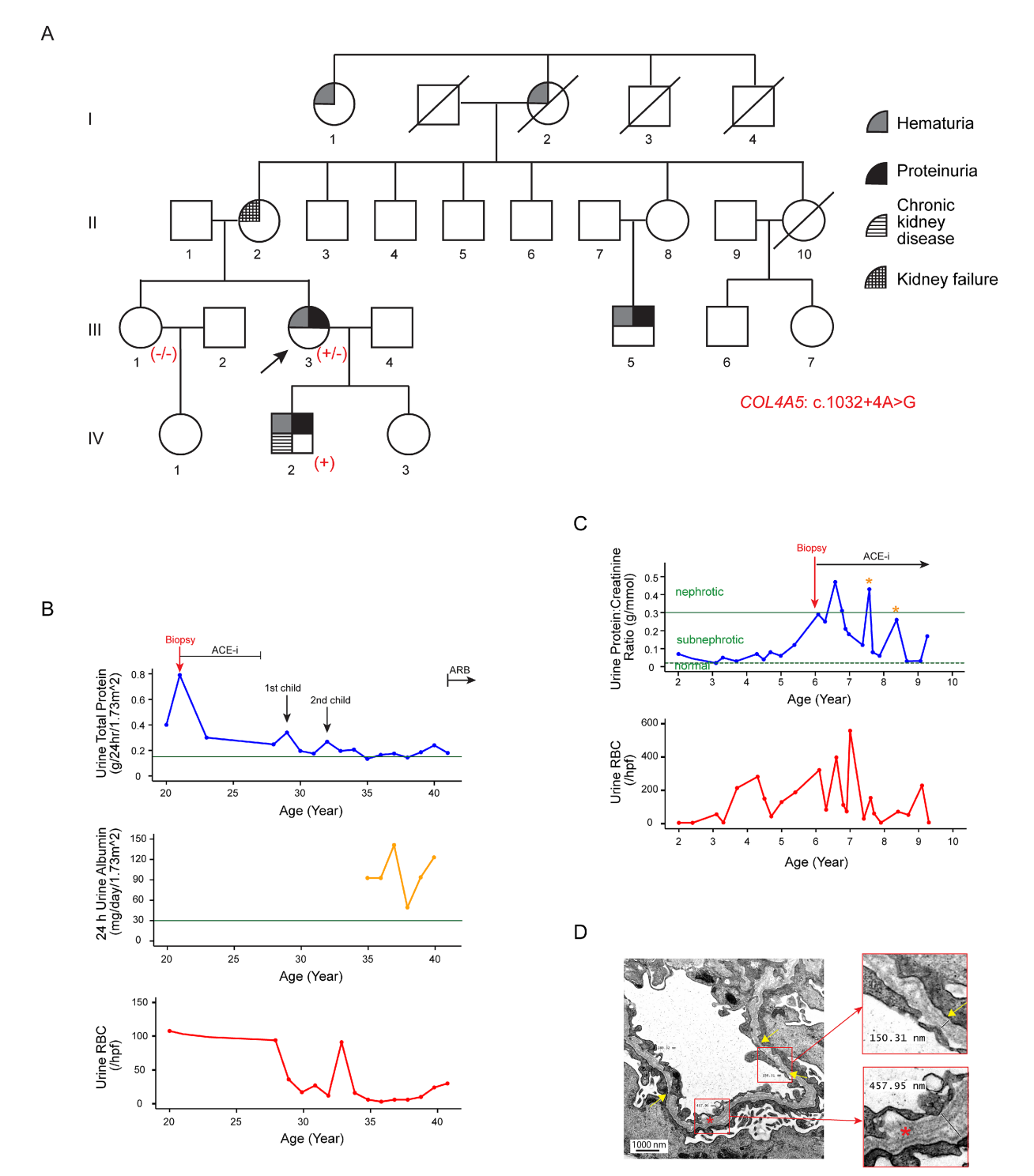
The proband's son (IV-2) displayed persistent microscopic hematuria (up to 56 RBCs/hpf) and subnephrotic proteinuria (urine protein-to-creatinine ratio 0.07 g/mmol) from the age of two (Figure 1C). His eGFR was normal at the initial presentation. He was given ACE-i from age six. His CKD had progressed to KDIGO stage G2A2 by the age of 9 years. A hearing assessment at age six was normal.

The proband's maternal male cousin (III-5) first presented at the age of 33 with incidental microscopic hematuria during health screening. Urine analysis revealed 10 RBCs/hpf, 60% of which were dysmorphic, along with normal albuminuria and preserved eGFR. Kidney ultrasound scans were unremarkable. He defaulted on follow-up but re-presented at the age of 44 with A2 albuminuria, although his eGFR remained normal. Ocular and audiological assessments at that time were normal.

In addition, the proband's grandaunt (I-1), aged 80, reportedly had hematuria and/or proteinuria, but further clinical details were unavailable.

Family B

The proband (IV-2; Figure 2A) first presented at the age of three with recurrent synpharyngitic gross hematuria and was subsequently found to have persistent microscopic hematuria (70 RBCs/hpf with 75% being dysmorphic). Subnephrotic proteinuria was noted, with a urine protein-to-creatinine ratio of 0.05 g/mmol. His eGFR was normal, and his autoimmune screen was negative. The patient was initially treated with cyclosporine A; however, this was discontinued

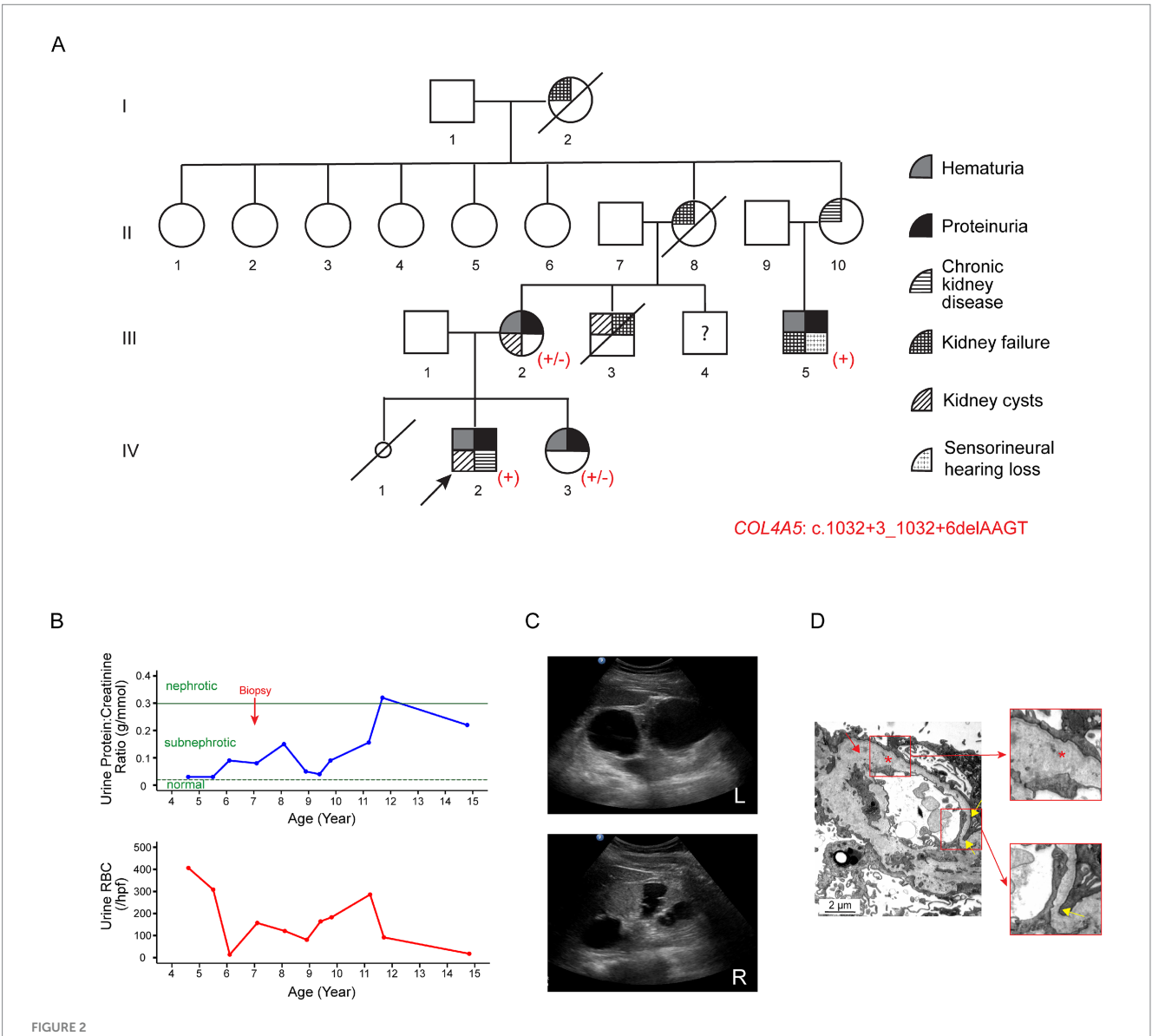


Clinical features of Family A associated with the variant c.1032 + 4A > G in COL4A5. (A) Pedigree of the affected family. Family members are denoted by generations I-IV. The arrow marks the proband; a slash strikethrough indicates deceased individuals. Genotypes are shown as -/- for non-carriers, +/- for heterozygous female individuals, and + for hemizygous male individuals carrying the variant. (B) Disease progression in the proband (III-3). The 24-h urinary total protein (g/day/body surface area 1.73m²), 24-h urinary albumin (mg/day/body surface area 1.73m²), and urine red blood cell count (RBCs/hpf) are displayed against age in years. The green horizontal lines in the upper and middle panels indicate the cutoff values for KDIGO categories A3 (24-h urine total protein, 0.15 g/day) and A2 (24-h urine albumin, 30 mg/day) albuminuria, respectively. (C) Disease progression in the proband's son (IV-2). The urine protein-to-creatinine ratio (g/mmol) and urinary red blood cell count (RBCs/hpf) are displayed against age in years. He exhibited persistent microscopic hematuria and subnephrotic proteinuria from the age of two. ACE-i therapy was initiated at age six following a kidney biopsy suggestive of Alport syndrome. The two yellow asterisks indicate episodes of viral infections associated with transient worsening of proteinuria. The green horizontal dotted and solid lines represent the cutoff values for sub-nephrotic (urine protein:creatinine ratio: 0.02 g/mmol) and nephrotic (urine protein:creatinine ratio: 0.03 g/mmol) proteinuria, respectively. (D) Representative electron microscopy images from the kidney biopsy of the proband's

(Continued)

FIGURE 1 (Continued)

son (IV-2). Electron microscopy revealed significant variability in GBM thickness, with alternating regions of thinning (\sim 150 nm; yellow arrows and upper insert) and thickening (\sim 460 nm; lower insert). The normal GBM thickness for a 6-year-old male individual ranges from 198 to 371 nm (15). The lamellated and irregular morphology of the GBM (red asterisk and lower insert) is highly indicative of Alport syndrome. In addition, the overlying podocyte foot processes were blunted and partially effaced.



Clinical features of Family B associated with the variant c.1032 + 3_1032 + 6delAAGT in COL4A5. (A) Pedigree of the affected family. Family members are denoted by generations I-IV. The arrow marks the proband; a slash strikethrough indicates deceased individuals; the smaller circle denotes a stillborn female baby. Genotypes are shown as +/- for heterozygous female individuals and + for hemizygous male individuals carrying the variant. (B) Disease progression in the proband (IV-2). The urine protein-to-creatinine ratio (g/mmol) and urinary red blood cell count (RBCs/hpf) are displayed against age in years. The proband first presented at the age of three with recurrent synpharyngitic gross hematuria and was subsequently found to have persistent microscopic hematuria. Subnephrotic proteinuria was also noted. The green horizontal dotted and solid lines represent the cutoff values for sub-nephrotic (urine protein-to-creatinine ratio: 0.02 g/mmol) and nephrotic (urine protein-to-creatinine ratio: 0.3 g/mmol) proteinuria, respectively. (C) Kidney ultrasound of the proband at the age of 15. Multiple large bilateral kidney cysts were observed, with the largest cyst in the right kidney measuring 2.7 cm x 3.4 cm and the largest in the left kidney measuring 5.0 cm x 5.3 cm. Upper panel: left kidney; lower panel: right kidney. (D) Representative electron microscopy images from the kidney biopsy of the proband's maternal uncle (III-5). The GBM featured alternating thickened segments (~769 nm to 1,244 nm) and thinning regions (~153 nm; yellow arrows and lower insert). The normal GBM thickness for a 15-year-old male individual ranges from 230 to 430 nm (15). The lamina densa displayed textural irregularities with some degree of lamellation and splitting (red asterisk and upper insert), suggestive of Alport syndrome.

due to the progressive decline in kidney function. Due to this, ACE-i therapy was commenced (Figure 2B). Notably, a kidney ultrasound performed at age 15 revealed bilateral echogenic kidneys, with the

right and left kidneys measuring 10.7 cm and 13.8 cm in length, respectively. Multiple large bilateral kidney cysts were observed, with the largest cyst in the right kidney measuring 2.7 cm x 3.4 cm and the

largest cyst in the left kidney measuring 5.0 cm x 5.3 cm (Figure 2C). Audiological assessments performed at the same age were normal. At present, aged 16, the proband's kidney function has progressively deteriorated to KDIGO stage G4A3.

The proband's mother (III-2) first presented at age 24 with persistent microscopic hematuria and proteinuria (Figure 2A). At age 26, she was found to have bilateral kidney cysts with septations. Kidney biopsy revealed focal segmental glomerulosclerosis (FSGS). During pregnancy, she developed pre-eclampsia, and an audiological evaluation at that time detected hearing loss. At the current age of 44, her eGFR remains within normal limits.

The proband's sister (IV-3) was found to have persistent hematuria (up to 60 RBCs/hpf) and subnephrotic proteinuria (0.5 g/day/1.73m²) at the age of seven. She was initiated on ACE-i therapy, and her eGFR has remained within normal limits.

The proband's distant maternal uncle (III-5), currently 28 years old, presented with persistent nephrotic-range proteinuria at age 15. At the initial presentation, his eGFR was 71 mL/min/1.73m². Kidney biopsy was suggestive of Alport syndrome (see Histological examination below). He subsequently progressed to kidney failure in his third decade of life and underwent kidney transplantation. In addition, he had bilateral sensorineural hearing loss.

Other maternal family members, including the proband's maternal uncle (III-3), grandmother (II-8), grandaunt (II-10), and maternal great-grandmother (I-2), had a history of chronic kidney disease and/or kidney failure requiring kidney replacement therapy.

Light and electron microscopy examinations of the kidney samples

Family A

A kidney biopsy was performed on the proband (III-3) at age 21 due to the presence of A3 albuminuria. A total of 30 glomeruli were examined. Light microscopy revealed a mild increase in the mesangial matrix without mesangial hypercellularity. Electron microscopy showed effacement of podocyte foot processes. The GBM exhibited areas of variable thinning and thickening, with occasional segments displaying lamination. Irregular lucencies were observed within the lamina rara interna, accompanied by scattered microparticles along the GBM.

The proband's son (IV-2) underwent a kidney biopsy at age six following the development of nephrotic-range proteinuria. A total of 20 glomeruli were examined. Light microscopy showed generally normocellular glomeruli with patent capillary lumina and predominantly single-contoured capillary walls, although there were segments of ischemic wrinkling. Two glomeruli displayed small segments of accentuated wrinkling, albeit without established sclerosis. Electron microscopy revealed significant variability in GBM thickness, with alternating regions of thinning (~150 nm) and thickening (~457 nm), along with the characteristic "basket-weaving" appearance in the thickened region (Figure 1D) (Normal GBM thickness for a 6-year-old male individual ranges from 198 to 371 nm) (15). This lamellated and irregular morphology of the GBM is highly indicative of Alport syndrome.

Family B

A kidney biopsy was performed on the proband (IV-2) at age seven when he had subnephrotic proteinuria with a normal eGFR. A total of 52 glomeruli were obtained. Light microscopic examination revealed generally normocellular glomeruli, with three glomeruli showing segmental mesangial hypercellularity. The capillary loops were patent, without the evidence of double-contoured capillary walls. There was focal mild tubular atrophy. Ultrastructural evaluation by electron microscopy showed diffuse and global thinning of the GBM, with basement membrane thickness across various capillary loops ranging from 122 nm to 201 nm (normal GBM thickness for 7-year-old male individuals ranges from 209 to 391 nm) (15). Podocyte foot process effacement was present, accompanied by microvillous transformation of the podocyte findings cytoplasm. These were consistent with GBM nephropathy.

The proband's maternal uncle (III-5) underwent a kidney biopsy at age 15 when he had KDIGO stage G2A3. A total of 16 glomeruli were sampled. Light microscopy showed that most glomeruli displayed wrinkling of capillary loops and basement membranes with textural irregularities, double-contoured segments, and occasional vacuolations. Mild mesangial expansion with increased cellularity was also noted. Electron microscopy showed the GBM with alternating thickened segments (~769 nm to 1,244 nm) and thinning portions (~153 nm to 268 nm) (normal GBM thickness for a 15-year-old male individual ranges from 230 to 430 nm) (15). In addition, the lamina densa exhibited textural irregularities with areas of lamellation and splitting (Figure 2D).

Exome sequencing of the probands

Genomic DNA was extracted from leukocytes, and exome sequencing was performed. The results revealed a heterozygous variant in COL4A5 [NM_000495.5]: c.1032 + 4A > G in the proband of Family A (III-3) and a hemizygous four-nucleotide deletion in COL4A5 [NM_000495.5]: $c.1032 + 3_{1032} + 6delAAGT$ in the proband of Family B (IV-2). The variants are located within intron 18 of the COL4A5 gene, proximal to the boundary between exon 18 and intron 18. Both variants are absent in population databases (Genome Aggregation Database; gnomAD v4.1.0). As shown in **Table** Supplementary COL4A5: c.1032 + 3_1032 + 6delAAGT is predicted to strongly disrupt the donor site, with scores of 1.00 and 0.86 and a shift from 8 to -19.72by SpliceAI (16), Pangolin (17), and MaxEnt (18, 19), respectively. In contrast, the variant COL4A5: c.1032 + 4A > G is predicted to moderately affect splicing, with scores of 0.46 and a shift from 8 to 2.94 by Pangolin and MaxEnt, respectively. This evidence suggests that these variants, located at non-canonical splice sites, are predicted to disrupt splicing by breaking the natural splice donor motif.

Familial segregation of the genetic variants

To further evaluate the pathogenicity of the variants, a detailed pedigree tree was drawn and the phenotypes for the family members

were obtained where possible. Sanger sequencing for the variant COL4A5: c.1032 + 4A > G was performed in Family A for individuals III-1 (sister) and IV-2 (son). The variant was detected in IV-2, who had progressed to KDIGO stage G2A2 by the age of 9 years, but it was absent in III-1, who exhibited no clinical evidence of kidney disease (Figure 1A). Similarly, Sanger sequencing for the variant COL4A5: c.1032 + 3_1032 + 6delAAGT was performed in Family B for members III-2 (mother), III-5 (maternal uncle), and IV-3 (sister). This variant was identified in all three family members, each displaying varying degrees of kidney disease severity (Figure 2A).

Immunofluorescence analysis of the kidney samples

In view of the electron microscopy changes seen in the kidney sample of the proband's son (IV-2) in Family A, immunofluorescence staining for collagen IV $\alpha 5$ was performed. This demonstrated interrupted, mosaic staining patterns along the GBM and distal tubular basement membrane (TBM), with significantly diminished or absent patterns in Bowman's capsule (Figure 3B). In contrast, control kidney tissue exhibited uniform, continuous staining of collagen IV $\alpha 5$ across the GBM, TBM, and Bowman's capsule (Figure 3A).

Similarly, immunofluorescence staining for collagen IV $\alpha 5$ was performed on the kidney tissue of the proband (IV-2) in Family B. This exhibited an abnormal mosaic and mildly diminished pattern along the GBM and Bowman's capsule, with a complete absence of staining along the distal TBM (Figure 3C). Immunofluorescence for collagen IV $\alpha 5$ in the proband's maternal uncle (III-5) from Family B also showed absence of staining in the GBM, Bowman's capsule, and distal TBM.

Minigene splicing assay

A minigene splicing assay was conducted to evaluate the impact of these non-canonical splice site variants on pre-messenger RNA

(mRNA) splicing and transcriptional outcomes. Briefly, the wildtype (WT) genomic sequence of COL4A5 (hg38: chrX-108,582,886-108,586,715), encompassing exons 17 to 19 and flanking introns 17 and 18, was amplified from the peripheral blood leukocytes of a healthy individual and subsequently cloned into the pcDNA3.4 expression vector to generate a wild-type control plasmid. The two mutant constructs were created by introducing the respective variants into the wild-type plasmid via site-directed mutagenesis (Figure 4A). The constructed plasmids were transfected into HEK293 cells, and total RNA was extracted 4 h post-transfection. Reverse-transcribed complementary DNA (cDNA) was used as a template for the amplification of transgene-derived transcripts with vector-specific primers. The wild-type construct yielded an intense band approximately 300 bp in size (Figure 4B). Conversely, the mutant plasmids harboring either variant generated a truncated transcript. Sanger sequencing of the purified polymerase chain reaction (PCR) products confirmed that the transcripts derived from the mutant plasmids exhibited exon 18 skipping (Figure 4C). Collectively, these findings demonstrate that both splice site variants lead to aberrant splicing, thereby confirming their functional impact.

Classification of the variants

Variant interpretation and classification were conducted in accordance with the guidelines of the ACMG/AMP (14, 20). These criteria were subsequently converted into quantitative point values (21) and integrated into a Bayesian framework for variant interpretation (22). The minigene splicing assay demonstrated that both variants caused aberrant splicing, leading to the skipping of exon 18, thereby fulfilling the criterion for PVS1_strong (23). When considered alongside additional lines of evidence, including minor allele frequencies from population databases, specific phenotype features such as pathological findings, and co-segregation among the family members, both variants met the threshold for reclassification

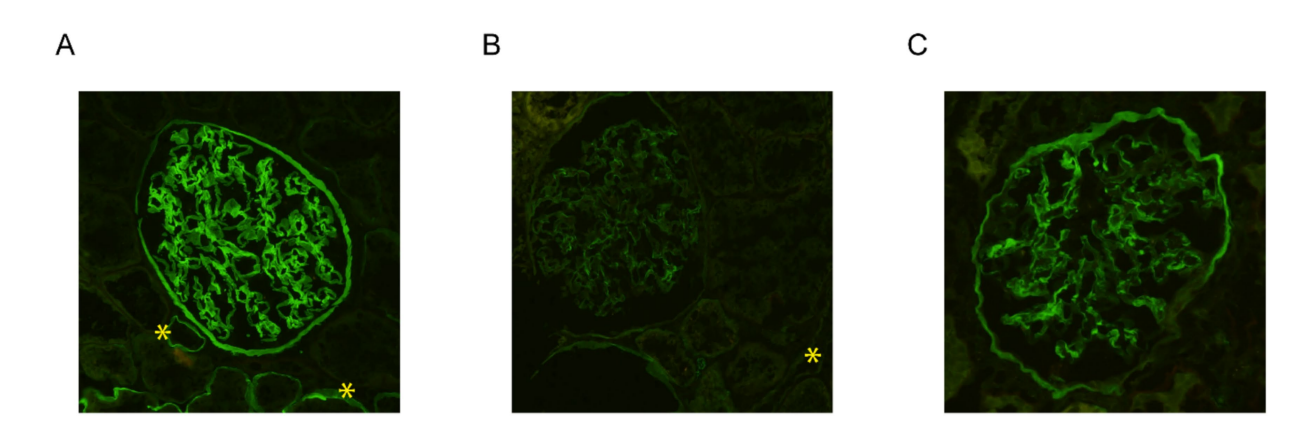
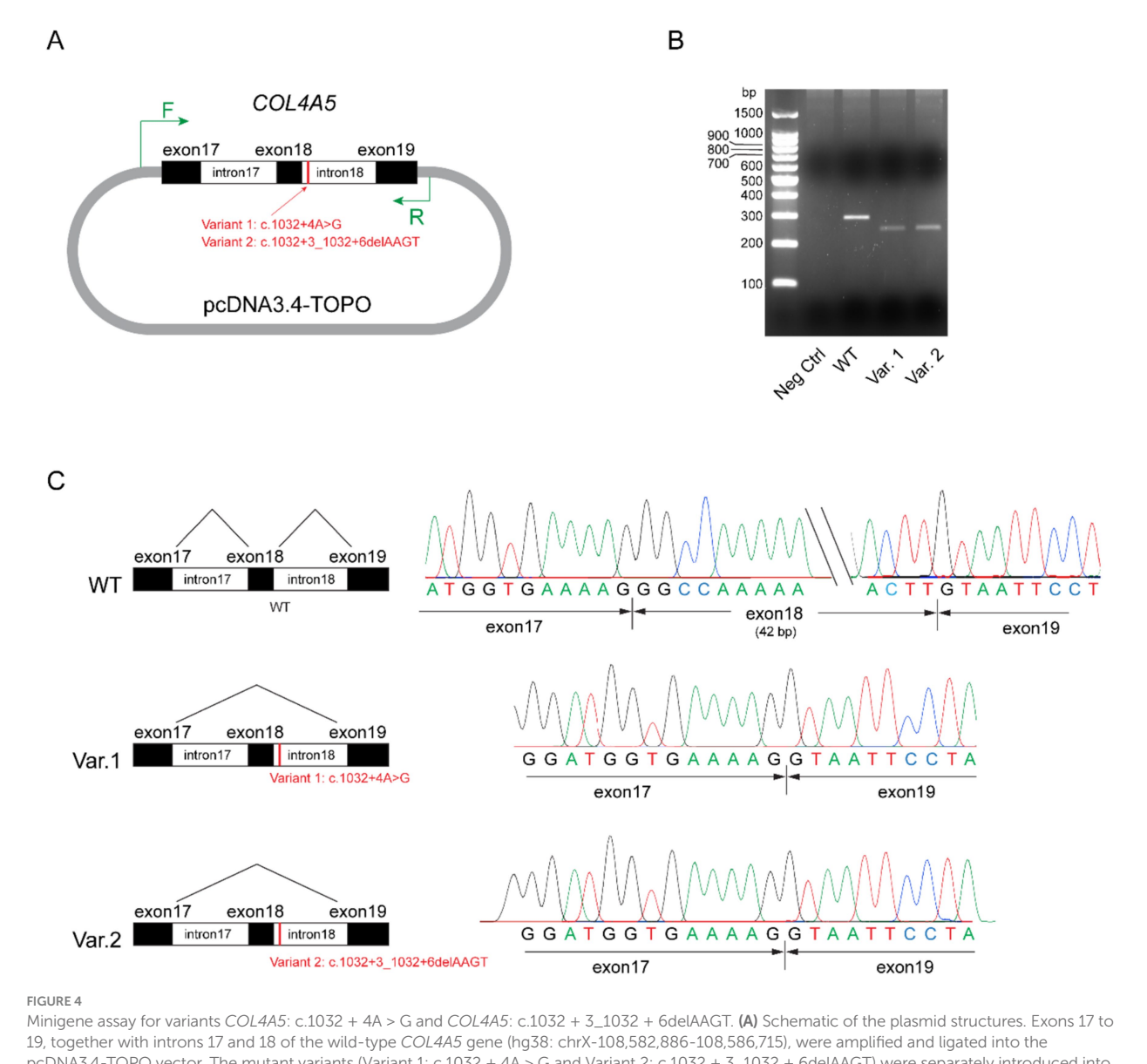


FIGURE 3 Immunofluorescence staining for collagen IV $\alpha 5$ in the kidney biopsy samples. While the control kidney tissue exhibited uniform, continuous staining of collagen IV $\alpha 5$ across the glomerular basement membrane (GBM), distal tubular basement membrane (TBM), and Bowman's capsule **(A)**, immunofluorescence staining of the kidney tissue from the proband's son in family A (IV-2) demonstrated an interrupted, mosaic staining pattern along the GBM and TBM, with significantly diminished or absent staining in Bowman's capsule **(B)**. Immunostaining analysis of the kidney tissue from the proband in family B (IV-2) exhibited an abnormal mosaic and mildly diminished pattern along the GBM and Bowman's capsule, with a complete absence of staining along the distal TBM **(C)**. Distal TBMs are marked with yellow asterisks. All three images were taken at 200x magnification.



Minigene assay for variants *COL4A5*: c.1032 + 4A > G and *COL4A5*: c.1032 + 3_1032 + 6delAAGT. (A) Schematic of the plasmid structures. Exons 17 to 19, together with introns 17 and 18 of the wild-type *COL4A5* gene (hg38: chrX-108,582,886-108,586,715), were amplified and ligated into the pcDNA3.4-TOPO vector. The mutant variants (Variant 1: c.1032 + 4A > G and Variant 2: c.1032 + 3_1032 + 6delAAGT) were separately introduced into the control plasmids through site-directed mutagenesis. The short vertical red line marks the variant loci, while the green arrows indicate primer pairs targeting vector-specific regions for polymerase chain reaction (PCR) amplification. (B) Agarose gel analysis of transgene transcripts. Total RNA was extracted from transfected HEK293 cells and reverse transcribed into cDNA. Transgene transcripts were amplified using primers targeting vector-specific regions, with cDNA as the template. While the negative control (pcDNA3.4-TOPO vector) did not yield any observable bands on the agarose gel (lane 2), the plasmid containing the wild-type (WT) form of exons 17 to 19 of *COL4A5* produced an intense band approximately 300 bp in size (lane 3). Plasmids harboring Variants (Var) 1 and 2 generated truncated transcripts, as evidenced by faint bands ranging from 200 bp to 300 bp (lanes 4 and 5). (C) Sanger sequencing results of the PCR products. Transcripts from the plasmid carrying the wild-type (WT) sequence included exons 17, 18, and 19 (top panel), whereas transcripts from plasmids carrying Variants 1 and 2 exhibited the skipping of exon 18 (middle and bottom panels, respectively).

as "Pathogenic" under the ACMG/AMP guidelines (see Supplementary Results and Supplementary Table S2).

Discussion

Interpretation of VUSs is a challenge in clinical genomic medicine, and this problem is exacerbated in the Asian population, which is underrepresented in genomic population-based databases (9). In this study, we demonstrated the use of the minigene assay, in conjunction with other lines of evidence such as immunofluorescence analysis of

kidney biopsies and familial segregation, to upgrade two non-canonical splice VUSs in the COL4A5 gene to 'Pathogenic' based on the ACMG / AMP criteria. Functionally, we demonstrated that both VUSs within intron 18 of the COL4A5 gene, c.1032 + 4 A > G and c.1032 + 3_1032 + 6delAAGT, can result in the skipping of exon 18 and consequently create a transcript with a 42-bp deletion.

Splicing is the process of removing RNA sequences transcribed from intronic DNA regions and joining the remaining exonic regions to form mRNA, which is required for protein synthesis. This process requires proper intron recognition and spliceosome assembly and is facilitated by conserved regulatory sequences located at the intron/

exon boundaries. The majority of introns are flanked by a GT dinucleotide at the 5' end and an AG dinucleotide at the 3' end (GT-AG). These are known as canonical splice sites at the intron/exon boundaries.

Disruptions in pre-mRNA splicing are an important pathomechanism in genetic disease—it is estimated that one-third of pathogenic variants cause aberrant splicing (24). Canonical splice site variants have been categorized as "very strong" diagnostic candidates in disorders where loss of function is a known disease mechanism (14). The role of variants in non-canonical splice sites, such as deep intronic variants or substitutions in exons, is also increasingly recognized. Exonic variants can interfere with splicing regulatory elements, resulting in exon skipping, while intronic variants can result in cryptic splice sites or cause retention of intronic fragments (25, 26). In exome sequencing data, 27% of pathogenic splicing variants are non-canonical. In XLAS, up to 18% of pathogenic *COL4A5* variants are splicing variants, and non-canonical splicing variants have also been reported (26).

In addition to the non-detection of deep intronic splice site variants by conventional sequencing techniques, clinical interpretation of non-canonical splice site variants is also challenging because there is often the need to demonstrate aberrant splicing as an additional piece of evidence to prove pathogenicity. Hence, transcriptional analysis is often required to facilitate re-classification of these variants.

Variant interpretation is highly variable, despite the availability of standard ACMG/AMP guidelines. For example, the variant *COL4A5*: c.1032 + 4A > C described in Family B has been previously reported in a 36-year-old male patient (27). This was classified as "pathogenic or likely pathogenic" based on the criteria of PP3_Very Strong and PM2_Supporting, although these two pieces of evidence may not be enough for one to designate a "Likely Pathogenic" criterion based on the ACMG/AMP guidelines and recent Bayesian framework (14, 20, 22). In ClinVar, this same variant (Variation ID: 2616665) was classified as a VUS (single submission). The variant COL4A5: c.1032 + 3_1032 + 6delAAGT found in Family A has been reported in a 10-year-old male patient with chronic kidney disease stage 2 (28), a patient with kidney failure at 26 years old (29), and a 12-year-old male patient with no further phenotype details (30). Consistent with our results, the authors of the latter study showed that this variant causes exon 18 skipping. The vector expression system in the minigene assay of our study is different from the one previously reported. Since the variant (c.1032 + 4A > G) has never been studied before, both variants were included in our minigene assay. As both variants are located within the same splicing motif, incorporating the variant c.1032 + 3_1032 + 6delAAGT as "positive control" served to provide an internal benchmark.

The ideal way to functionally characterize a VUS predicted to involve splice sites is to conduct *in vivo* transcriptional analysis using the patients' affected tissues to examine tissue-specific gene expression (13). In the case of Alport syndrome, kidney biopsy samples are often not readily available for such studies. Alternative options include *in silico* splice prediction, but the sensitivity of this method is low (31). Transcription assays, such as the minigene assay, are useful for investigating aberrant splicing because they do not require tissue-specific biological samples and their results can be consistent with *in vivo* studies (11, 13, 30). Nevertheless, routine clinical use of transcription assays may be limited due to a lack of widespread expertise and the labor-intensive nature of these procedures.

Moreover, kidney cysts are increasingly reported in individuals with pathogenic variants in *COL4A3-COL4A5* and a diagnosis of Alport syndrome (3). These cysts, often appearing before age 50, are typically confined to the kidneys and are more commonly found in individuals with proteinuria, suggesting a link to more severe disease (4). While the kidney cysts are not large enough to cause direct renal decline, their presence may indicate disease progression. Recent studies have reported cysts in approximately 38% of genetically confirmed patients with Alport syndrome, with some showing increased kidney volume that can mimic autosomal dominant polycystic kidney disease (ADPKD) (5). As highlighted in the latest ERKNet guidelines (32), genetic testing for cystic kidney disease should include *COL4A3-COL4A5* to ensure accurate diagnosis and avoid misclassification.

We also described the use of immunofluorescence analysis for collagen IV $\alpha5$ in kidney tissues to substantiate the interpretation of VUSs. While classical features of electron microscopy of Alport syndrome can be adequate for a clinical diagnosis of Alport syndrome, such findings are often not present in the earlier stages of the disease (31, 33, 34). On the other hand, approximately 70–80% of male individuals with X-linked Alport syndrome exhibit absent staining for collagen IV $\alpha5$ chains (35). Consequently, immunofluorescence staining for type IV collagen can be invaluable for diagnostic purposes. The abnormal immunostaining of collagen IV $\alpha5$ may further support the evidence that these families carry phenotypes specific to this disease.

In conclusion, we demonstrate a structured evaluation approach for the reclassification of two previously reported VUSs by applying multiple ACMG /AMP guidelines, in accordance with the Bayesian framework. By implementing this VUS resolution program, we can systematically resolve variants with uncertain significance and increase diagnostic yield in genomic medicine within nephrology (36).

Data availability statement

The original contributions presented in the study are included in the article/Supplementary material; further inquiries can be directed to the corresponding authors.

Ethics statement

The studies involving humans were approved by Institutional Ethics Review Committee, Domain Specific Review Boards, National Healthcare Group (2022/00108). The studies were conducted in accordance with the local legislation and institutional requirements. The participants provided their written informed consent to participate in this study. Written informed consent was obtained from the individual(s) for the publication of any potentially identifiable images or data included in this article.

Author contributions

CK: Data curation, Writing – original draft, Writing – review & editing, Resources. TL: Writing – review & editing, Investigation, Methodology, Writing – original draft. AL: Investigation,

Methodology, Writing - review & editing. YN: Methodology, Writing - review & editing, Investigation. JK: Writing - review & editing, Data curation, Investigation. PL: Writing - review & editing, Investigation. HC: Data curation, Writing - review & editing. JN: Investigation, Writing - review & editing, Data curation, Resources. MT: Data curation, Writing - review & editing, Investigation, Resources. IM: Writing - review & editing. CL: Investigation, Writing - review & editing. KC: Writing - review & editing. JC: Investigation, Writing - review & editing. HY: Writing - review & editing, Investigation. KN: Investigation, Writing - review & editing, Conceptualization, Funding acquisition, Methodology, Project administration, Resources, Supervision, Validation, Visualization, Writing - original draft, Data curation. YZ: Investigation, Writing review & editing, Conceptualization, Data curation, Methodology, Supervision, Validation, Visualization, Writing - original draft, Project administration.

Funding

The author(s) declare that financial support was received for the research and/or publication of this article. This project is supported by Renal Alliance for PrecIsion Diagnosis in Singapore (RAPIDS), which is funded by the National Research Foundation, Singapore, through the Singapore Ministry of Health's National Medical Research Council and the Precision Health Research, Singapore (PRECISE), under PRECISE's Clinical Implementation Pilot grant scheme; by the National Precision Medicine Programme (NPM) PHASE II FUNDING to LWK (MOH-000588); and by the Clinician Scientist Individual Research Grant to NKH (MOH-001485-00) from National Medical Research Council, Singapore (NMRC).

References

- 1. Groopman EE, Marasa M, Cameron-Christie S, Petrovski S, Aggarwal VS, Milo-Rasouly H, et al. Diagnostic utility of exome sequencing for kidney disease. *N Engl J Med.* (2019) 380:142–51. doi: 10.1056/NEJMoa1806891
- 2. Watson S, Padala SA, Hashmi MF, Bush JS. Alport Syndrome. Treasure Island, FL: StatPearls (2024).
- 3. Savige J, Mack H, Thomas R, Langsford D, Pianta T. Alport syndrome with kidney cysts is still Alport syndrome. *Kidney Int Rep.* (2022) 7:339–42. doi: 10.1016/j.ekir.2021.11.004
- 4. Sevillano AM, Gutierrez E, Morales E, Hernandez E, Molina M, Gonzalez E, et al. Multiple kidney cysts in thin basement membrane disease with proteinuria and kidney function impairment. *Clin Kidney J.* (2014) 7:251–6. doi: 10.1093/ckj/sfu033
- 5. Zeni L, Mescia F, Toso D, Dordoni C, Mazza C, Savoldi G, et al. Clinical significance of the cystic phenotype in Alport syndrome. *Am J Kidney Dis.* (2024) 84:320–328.e1. doi: 10.1053/j.ajkd.2024.02.005
- 6. Fogo AB, Lusco MA, Najafian B, Alpers CE. AJKD atlas of renal pathology: Alport syndrome. *Am J Kidney Dis.* (2016) 68:e15–6. doi: 10.1053/j.ajkd.2016.08.002
- 7. Zeng M, di H, Liang J, Liu Z. Effectiveness of renin-angiotensin-aldosterone system blockers in patients with Alport syndrome: a systematic review and meta-analysis. *Nephrol Dial Transplant.* (2023) 38:2485–93. doi: 10.1093/ndt/gfad105
- 8. Kashtan CE, Gross O. Clinical practice recommendations for the diagnosis and management of Alport syndrome in children, adolescents, and young adults-an update for 2020. *Pediatr Nephrol.* (2021) 36:711–9. doi: 10.1007/s00467-020-04819-6
- 9. Chen E, Facio FM, Aradhya KW, Rojahn S, Hatchell KE, Aguilar S, et al. Rates and classification of variants of uncertain significance in hereditary disease genetic testing. *JAMA Netw Open.* (2023) 6:e2339571. doi: 10.1001/jamanetworkopen.2023.39571
- 10. Walsh N, Cooper A, Dockery A, O'Byrne JJ. Variant reclassification and clinical implications. *J Med Genet*. (2024) 61:207–11. doi: 10.1136/jmg-2023-109488

Conflict of interest

The authors declare that the research was conducted in the absence of any commercial or financial relationships that could be construed as a potential conflict of interest.

Generative AI statement

The authors declare that no Gen AI was used in the creation of this manuscript.

Any alternative text (alt text) provided alongside figures in this article has been generated by Frontiers with the support of artificial intelligence and reasonable efforts have been made to ensure accuracy, including review by the authors wherever possible. If you identify any issues, please contact us.

Publisher's note

All claims expressed in this article are solely those of the authors and do not necessarily represent those of their affiliated organizations, or those of the publisher, the editors and the reviewers. Any product that may be evaluated in this article, or claim that may be made by its manufacturer, is not guaranteed or endorsed by the publisher.

Supplementary material

The Supplementary material for this article can be found online at: https://www.frontiersin.org/articles/10.3389/fmed.2025.1611334/full#supplementary-material

- 11. Horinouchi T, Nozu K, Yamamura T, Minamikawa S, Nagano C, Sakakibara N, et al. Determination of the pathogenicity of known COL4A5 intronic variants by in vitro splicing assay. *Sci Rep.* (2019) 9:12696. doi: 10.1038/s41598-019-48990-9
- 12. Gaildrat P, Killian A, Martins A, Tournier I, Frébourg T, Tosi M. Use of splicing reporter minigene assay to evaluate the effect on splicing of unclassified genetic variants. *Methods Mol Biol.* (2010) 653:249–57. doi: 10.1007/978-1-60761-759-4 15
- 13. Lord J, Baralle D. Splicing in the diagnosis of rare disease: advances and challenges. Front Genet. (2021) 12:689892. doi: 10.3389/fgene.2021.689892
- 14. Richards S, Aziz N, Bale S, Bick D, das S, Gastier-Foster J, et al. Standards and guidelines for the interpretation of sequence variants: a joint consensus recommendation of the American College of Medical Genetics and Genomics and the Association for Molecular Pathology. *Genet Med.* (2015) 17:405–24. doi: 10.1038/gim.2015.30
- 15. Haas M. Alport syndrome and thin glomerular basement membrane nephropathy: a practical approach to diagnosis. *Arch Pathol Lab Med.* (2009) 133:224–32. doi: 10.5858/133.2.224
- 16. Jaganathan K, Kyriazopoulou Panagiotopoulou S, McRae JF, Darbandi SF, Knowles D, Li YI, et al. Predicting splicing from primary sequence with deep learning. *Cell.* (2019) 176:535–548.e24. doi: 10.1016/j.cell.2018.12.015
- 17. Zeng T, Li YI. Predicting RNA splicing from DNA sequence using pangolin. Genome Biol. (2022) 23:103. doi: 10.1186/s13059-022-02664-4
- 18. Yeo G, Burge CB. Maximum entropy modeling of short sequence motifs with applications to RNA splicing signals. *J Comput Biol.* (2004) 11:377-94. doi: 10.1089/1066527041410418
- 19. Shamsani J, Kazakoff SH, Armean IM, McLaren W, Parsons MT, Thompson BA, et al. A plugin for the Ensembl variant effect predictor that uses MaxEntScan to predict variant spliceogenicity. *Bioinformatics*. (2019) 35:2315–7. doi: 10.1093/bioinformatics/bty960
- 20. Savige J, Storey H, Watson E, Hertz JM, Deltas C, Renieri A, et al. Consensus statement on standards and guidelines for the molecular diagnostics of Alport

syndrome: refining the ACMG criteria. Eur J Hum Genet. (2021) 29:1186–97. doi: 10.1038/s41431-021-00858-1

- 21. Tavtigian SV, Harrison SM, Boucher KM, Biesecker LG. Fitting a naturally scaled point system to the ACMG/AMP variant classification guidelines. *Hum Mutat.* (2020) 41:1734–7. doi: 10.1002/humu.24088
- 22. Tavtigian SV, Greenblatt MS, Harrison SM, Nussbaum RL, Prabhu SA, Boucher KM, et al. Modeling the ACMG/AMP variant classification guidelines as a Bayesian classification framework. *Genet Med.* (2018) 20:1054–60. doi: 10.1038/gim.2017.210
- 23. Abou Tayoun AN, Pesaran T, DiStefano MT, Oza A, Rehm HL, Biesecker LG, et al. Recommendations for interpreting the loss of function PVS1 ACMG/AMP variant criterion. *Hum Mutat.* (2018) 39:1517–24. doi: 10.1002/humu.23626
- 24. Lim KH, Ferraris L, Filloux ME, Raphael BJ, Fairbrother WG. Using positional distribution to identify splicing elements and predict pre-mRNA processing defects in human genes. *Proc Natl Acad Sci USA*. (2011) 108:11093–8. doi: 10.1073/pnas.1101135108
- 25. Jais JP, Knebelmann B, Giatras I, Marchi M, Rizzoni G, Renieri A, et al. X-linked Alport syndrome: natural history in 195 families and genotype- phenotype correlations in males. J Am Soc Nephrol. (2000) 11:649–57. doi: 10.1681/ASN.V114649
- 26. Yamamura T, Horinouchi T, Aoto Y, Lennon R, Nozu K. The contribution of COL4A5 splicing variants to the pathogenesis of X-linked Alport syndrome. *Front Med.* (2022) 9:841391. doi: 10.3389/fmed.2022.841391
- 27. Tato AM, Carrera N, García-Murias M, Shabaka A, Ávila A, Mora Mora MT, et al. Genetic testing in focal segmental glomerulosclerosis: in whom and when? *Clin Kidney J.* (2023) 16:2011–22. doi: 10.1093/ckj/sfad193
- $28.\,\mathrm{Li}$ S, Hu M, He C, Sun Y, Huang W, Lei F, et al. A multicenter study investigating the genetic analysis of childhood steroid-resistant nephrotic syndrome: variants in

- COL4A5 may not be coincidental. PLoS One. (2024) 19:e0304864. doi: 10.1371/journal.pone.0304864
- 29. Knebelmann B, Breillat C, Forestier L, Arrondel C, Jacassier D, Giatras I, et al. Spectrum of mutations in the COL4A5 collagen gene in X-linked Alport syndrome. *Am J Hum Genet*. (1996) 59:1221–32.
- 30. Horinouchi T, Nozu K, Yamamura T, Minamikawa S, Omori T, Nakanishi K, et al. Detection of splicing abnormalities and genotype-phenotype correlation in X-linked Alport syndrome. *J Am Soc Nephrol.* (2018) 29:2244–54. doi: 10.1681/ASN.2018030228
- 31. Zhang Y, Wang X, Zhou J, Ding J, Wang F. Abnormal mRNA splicing effect of COL4A3 to COL4A5 unclassified variants. *Kidney Int Rep.* (2023) 8:1399–406. doi: 10.1016/j.ekir.2023.04.001
- 32. Torra R, Lipska-Zietkiewicz B, Acke F, Antignac C, Becker JU, Cornec-le Gall E, et al. Diagnosis, management and treatment of the Alport syndrome 2024 guideline on behalf of ERKNet, ERA and ESPN. *Nephrol Dial Transplant*. (2025) 40:1091–106. doi: 10.1093/ndt/gfae265
- 33. Vischini G, Kapp ME, Wheeler FC, Hopp L, Fogo AB. A unique evolution of the kidney phenotype in a patient with autosomal recessive Alport syndrome. *Hum Pathol.* (2018) 81:229–34. doi: 10.1016/j.humpath.2018.02.024
- 34. Storey H, Savige J, Sivakumar V, Abbs S, Flinter FA. COL4A3/COL4A4 mutations and features in individuals with autosomal recessive Alport syndrome. *J Am Soc Nephrol.* (2013) 24:1945–54. doi: 10.1681/ASN.2012100985
- 35. Kashtan CE. Alport Syndrome- GeneReviews. Seattle: University of Washington (2001).
- 36. Lim C, Lim RS, Choo J, Leow EH, Chan GC, Zhang Y, et al. Clinical implementation of nephrologist-led genomic testing for glomerular diseases in Singapore: rationale and protocol. Am J Nephrol. (2024) 56:158-71. doi: 10.1159/000542942